Title:
Reduction in barreling of hollow cylinder by ram pulsation in upsetting

Authors:
Ryo Matsumoto[1,*], Yuya Monda[1] and Hiroshi Utsunomiya[1]

* Correspnding author (R. Matsumoto, E-mail: ryo@mat.eng.osaka-u.ac.jp, Tel: +81-6-6879-7500, Fax: +81-6-6879-7500)

Affiliation:
[1] Division of Materials and Manufacturing Science, Osaka University, 2-1 Yamadaoka, Suita 565-0871, Japan

Abstract

Barreling of hollow cylinder was investigated in cold upsetting with ram pulsation. In experiment of upsetting of 18Cr-12Ni-2.5Mo austenitic stainless steel (JIS: SUS316), barreling was reduced by complete unload ram pulsation, especially by multiple pulsations with short forming stroke. On the other hand, barreling was not reduced by ram pulsation with partial unloading. In case of hollow cylinder with pure aluminum (JIS: A1070), barreling was not reduced by both complete and partial unload ram pulsations. The mechanism of reduction in barreling was discussed from the viewpoints of friction at the die–workpiece contact interface, plastic heat generation, and elastic and plastic deformations. In the elastic-plastic finite element analysis, the stress state in the workpiece at reloading after complete unloading was considerably changed from that with the state before unloading. Therefore, the reduction in barreling in upsetting with complete unload ram pulsation was concluded to be mainly due to the elastic and plastic characteristics of the workpiece.

Keywords: Forging; Upsetting; Ram pulsation; Barreling; Pipe

1. Introduction

In response to strong demand for lightweight vehicles and complex shape of structural components, development of forming process for hollow component such as pipe, tube, and hollow rod, is crucial [1]. Several novel forming processes for hollow component are proposed [2-5]. Nonuniform, local deformations or plastic instability such as barreling, bending, and plastic bucking, tends to occur in upsetting of rod, especially hollow or long rod with high slenderness ratio (length/radius of gyration). Forming conditions of the hollow or long rod are strongly limited by such shape defects. Although the slenderness ratio of the rod is dominant for the defects [6], the defects are also induced by friction at die–workpiece contact interface, inhomogeneity, and anisotropy of rod material.

Simple conventional technique for the solution of the defects is friction reduction at die–workpiece contact interface [7], however, it is difficult to completely eliminate the friction by lubrication or die coating. Practical conventional techniques in industries are changes of process design and die shape, such as multi-stage forming and constraint of the outer and/or inner sections of the workpiece by the die. Some advanced techniques have been also proposed. For example, plastic buckling and fracture of a tube were reduced by pulsation of oil pressure in hydroforming [8]. A ring was expanded in radial direction by pressure of oil filled in the hollow space in axial compression [9]. Barreling of hollow cylinder was reduced by superposing compression and torsion in upsetting [10]. The hollow cylinder was successfully deformed without barreling and hourglass deformation under sequential control of torsion speed in upsetting with conical dies [11].

Barreling profile of cylindrical workpiece in compression has been fundamentally investigated through theoretical, numerical, and experimental approaches since the 1960s [12]. Especially the relationship between barreling and friction at die–workpiece contact interface is actively reported because the friction is dominant for barreling in compression [13-15].

Stress–strain relationship of the workpiece is inversely identified from the barreling–friction relationship [16,17]. Influences of strain hardening and strain rate on barreling are also reported in compression [18]. As barreling increases in compression with high friction or high reduction, folding of the workpiece at the die–workpiece needs to be taken into consideration [19]. Barreling and folding are affected by stress–strain relationship (including with inhomogeneity and anisotropy) as well as friction at die–workpiece contact interface.

Owing to the development of servo-drive press machines, the ram operations such as acceleration, deceleration, reversal, and holding were widespread as a helpful means for developing advanced forming processes in metal forming academia/industries [20,21]. Net/near net-shaping with complicated shape and high productivity with short forming cycle were realized by the ram operations under controlling temperature, friction, and load. Although the ram pulsation (oscillation, vibration) was fundamentally reported in forward extrusion for the purpose of load reduction in the 1970s before the development of the servo press [22], it has mainly developed into one of practical ram operations since the 2000s together with the development of the servo press. In the ram pulsation, the ram is repeatedly moved forward (advance) and backward (retreat) with low frequency (frequency: below approximately 100 Hz, amplitude: over approximately 0.1 mm), compared to the frequency of ultrasonic vibration. The contacting and loading/unloading conditions at die–workpiece contact interface induce some unique characteristics in friction, heat generation, and elastic-plastic deformation. The phenomena and industrial applications of forging with ram pulsation were reviewed [23]. The mechanisms of such phenomena caused by the ram pulsation were also discussed through experimental, numerical, and theoretical approaches. For example, periodical lubricant supply through a gap between die and workpiece [24-26] and plastic flow control by reduction in local plastic heat generation [27,28] were reported. On the other hand, ductility enhancement by stress relaxation [29] and reduction in

springback by elastic recovery [30] were reported in sheet metal forming. Most investigations on the characteristics induced by elastic-plastic stress change during ram pulsation have been reported in tensile stress field such as uniaxial tension and bending, while few investigations have been reported in compressive stress field such as upsetting and extrusion.

In this study, relationship between ram pulsation of press and barreling of hollow cylinder is investigated in experiment of cold upsetting. The stress state and deformation of the workpiece during ram retreat are analyzed by the elastic-plastic finite element analysis. The mechanism of reduction in barreling of the hollow cylinder is discussed from the viewpoints of friction at the die–workpiece contact interface, plastic heat generation, and elastic-plastic deformation.

2. Forging conditions and experimental procedures

2.1. Forging shape and materials

Figure 1 shows the schematic illustration of the layout of the workpiece and the dies in upsetting with ram pulsation. The hollow cylindrical workpiece with outer diameter of D_0 = ϕ15 mm, inner diameter of d_0 = ϕ12 mm, and height of h_0 = 15 mm or 10 mm (slenderness ratio: 3.1 or 2.1) was axially compressed between the upper and lower dies aligning the center axes in the axial direction (z direction). The dies were conical with a vertex angle of 179º in order to cause large barreling in the workpiece. Here, barreling (D_c/D_e) was defined as the outer diameter of the workpiece at the height center (D_c) divided with mean outer diameter of the workpiece at the top and bottom ends (D_e).

18Cr-12Ni-2.5Mo austenitic stainless steel (JIS: SUS316) with h_0 = 15 mm and commercially pure aluminum (JIS: A1070-H14, Al ≥ 99.7 mass%) with h_0 = 10 mm were used as the workpiece materials, while high-speed tool steel (JIS: SKH51, 63 HRC) was used as the die material. The workpiece materials are popular materials of pipe. The end surfaces of

the workpiece were machined to be arithmetic mean roughness of Ra = 2.7 μm, while the end surface of the dies was polished to be Ra = 0.02–0.04 μm (mirror-like finish). Upsetting was carried without lubrication at room temperature on a ball screw type material testing machine with servo motor driven. The translational speed and direction of the upper ram were controlled by the programmed operation.

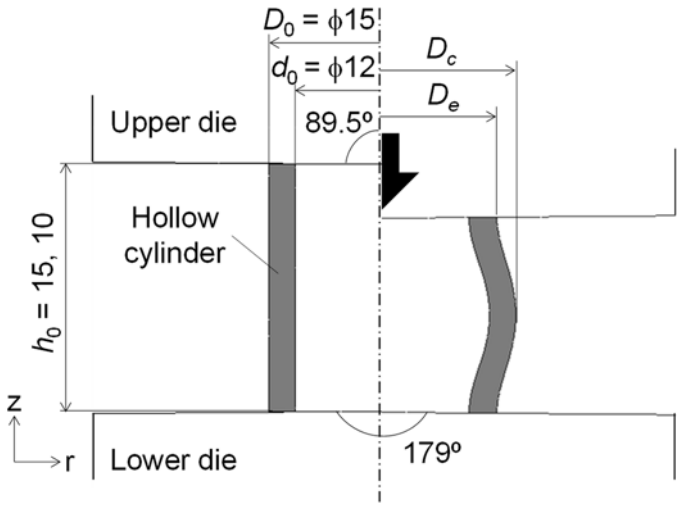

Fig. 1 Layout of hollow cylindrical workpiece and conical dies in upsetting with ram pulsation.

2.2 Pulsation ram motion

The ram position–time diagram of pulsation ram motion is shown in **Figure 2**. The upper ram of a press was advanced in the -z direction by repeatedly moving forward (advance) and backward (retreat). The upper die was synchronized with the ram. The workpiece was deformed during ram advance, while the load was released during ram retreat. As the results, the workpiece was intermittently deformed.

The ram speed in the ram advance and retreat was set to 1.0 mm/s in this study. The basic pulsation was set to start stroke of pulsation s_{f0} = 0.6 mm, retreat stroke in each pulsation s_r = 0.2 mm and 1.0 mm, and total forming stroke s_{total} (= s_{f0} + $s_f \cdot n_{total}$) = 3.0 mm for

h_0 = 15 mm and 2.0 mm for h_0 = 10 mm (n_{total}: total number of pulsation). According to the basic pulsation, the advance stroke in each pulsation (s_a), forming stroke in each pulsation (s_f (= $s_a - s_r$)), and n_{total} were determined to 0.3–3.4 mm, 0.1–2.4 mm, and 1–24, in respectively. Since the load was released by the ram retreat, the unload fraction ($\Delta f/f_0$) in the following equation was experimentally measured:

$$\Delta f/f_0 = \frac{f_0 - f_r}{f_0} \quad (1)$$

where f_0 and f_r are the forming loads at start and finish of the ram retreat, respectively. **Figure 3** shows the measurement results of the unload fraction in upsetting with ram pulsation. The load was released approximately half at s_r = 0.2 mm ($\Delta f/f_0$ = 0.4), while it was completely unloaded by the ram retreat with $s_r \geq 1.0$ mm ($\Delta f/f_0$ = 1). The complete unloading formed the gap between the top end of the workpiece and the end face of the upper die.

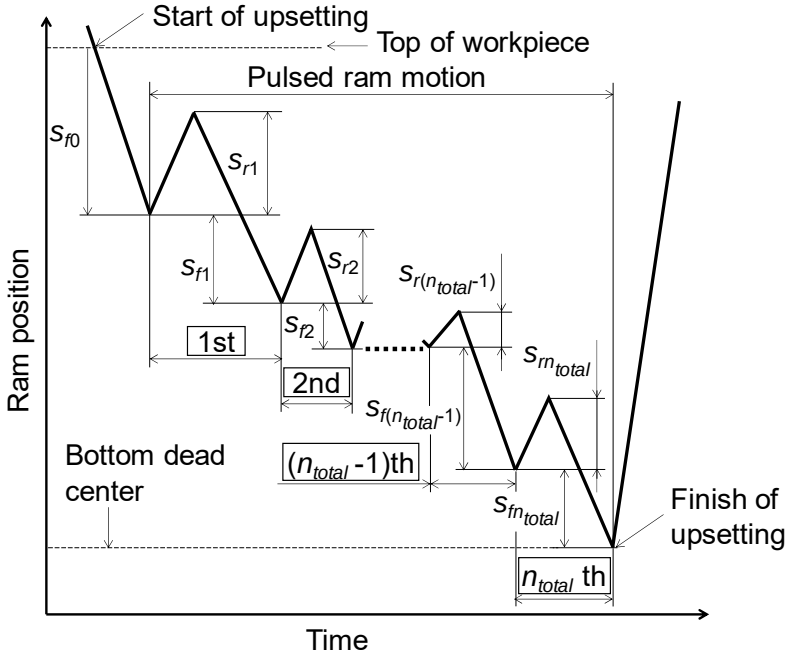

Fig. 2 Ram position–time diagram of pulsation ram in upsetting (s_{f0}: start stroke of pulsation, s_r (= s_{ri}): retreat stroke in each pulsation, s_a (= s_{ai}): advance stroke in each pulsation, s_f (= s_{fi}): forming stroke in each pulsation, n_{total}: total number of pulsation, i = 1–n_{total}).

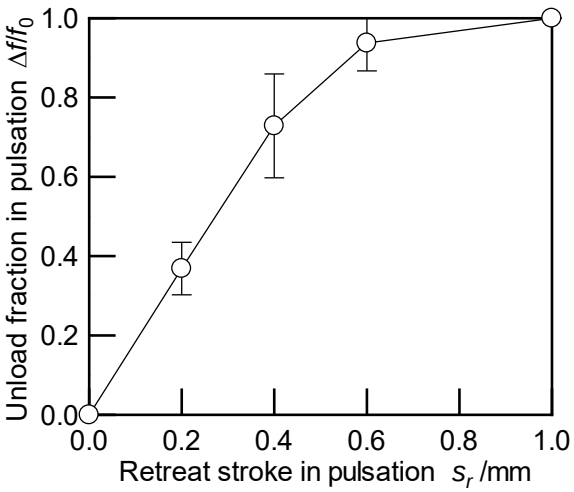

Fig. 3 Experimental results of relationship between unload fraction and retreat stroke in upsetting with ram pulsation.

3. Experimental results

3.1. Barreling of workpiece

Figure 4 shows the appearances of stainless steel workpieces after upsetting. Barreling of the workpiece occurred in upsetting with/without ram pulsation. The measurement results of the wall thickness of the workpiece after upsetting are shown in **Figure 5**. The wall thickness was overall thickened in upsetting with/without ram pulsation. In the workpieces without/with pulsation, the rθ cross-sectional areas of the top and bottom ends increased by approximately 10% from the initial, the cross-sectional areas of the height center increased by approximately 5% from the initial.

Figure 6 shows the relationship between barreling and reduction in height in upsetting of the stainless steel workpiece. Barreling with/without ram pulsation increased with increasing reduction in height. Barreling with pulsation was slightly lower than barreling without pulsation, and the reduction ratio was approximately 1.5% at $s_{total}/h_0 = 0.20$. The relationship between barreling and forming stroke per pulsation in upsetting is shown in

Figure 7. Barreling of the stainless steel workpiece was reduced with shorter forming stroke per pulsation in upsetting with s_r = 1.0 mm (complete unloading) (approximately 2.5% reduction in s_f/h_0 = 0.007), while barreling was not reduced by ram pulsation with s_r = 0.2 mm (partial unloading). The maximum reduction ratio was approximately 2.5% at s_{total}/h_0 = 0.20 in s_f/h_0 = 0.007. On the other hand, barreling of aluminum workpiece was not reduced even with s_r = 1.0 mm. From the results, the combination of stainless steel and complete unload ram pulsation is effective for reducing barreling.

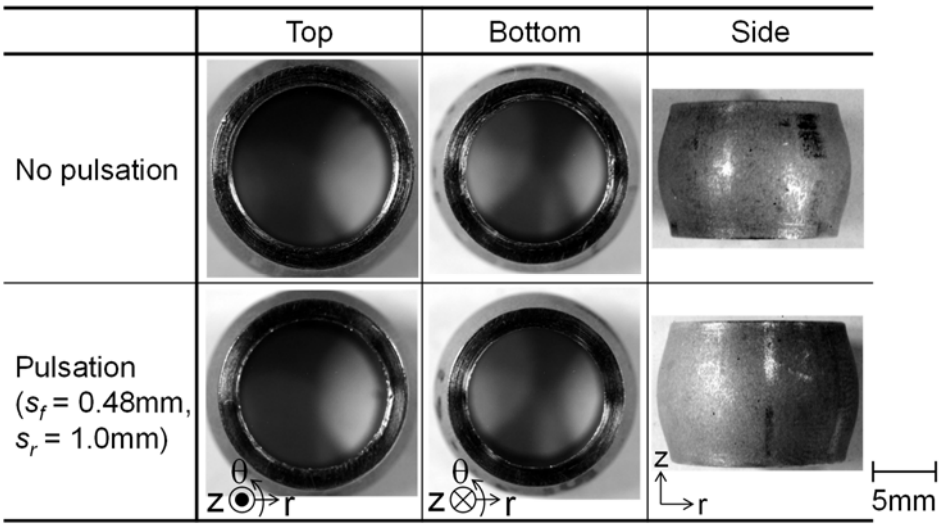

Fig. 4 Appearances of stainless steel workpieces after upsetting with/without ram pulsation (s_{total}/h_0 = 0.20).

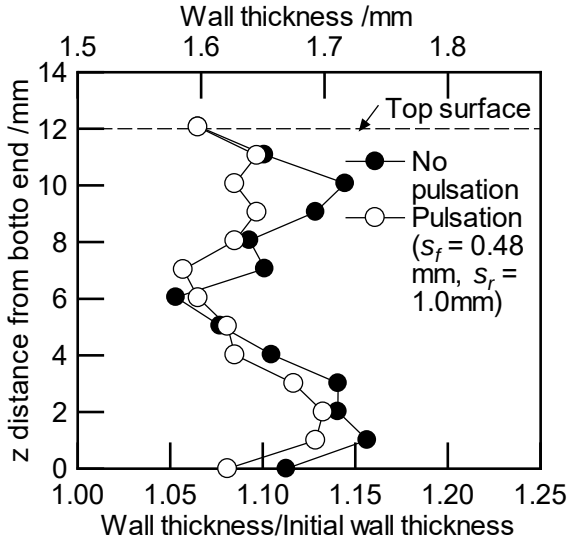

Fig. 5 Wall thickness of stainless steel workpiece after upsetting with/without ram pulsation (s_{total}/h_0 = 0.20).

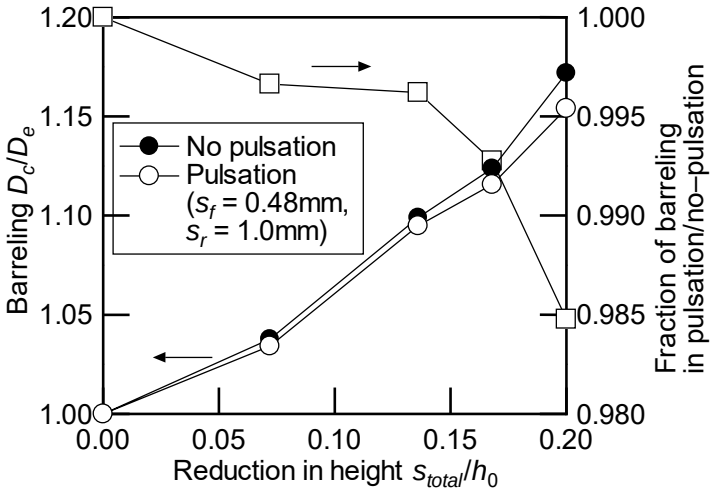

Fig. 6 Relationship between barreling and reduction in height in upsetting of stainless steel workpiece.

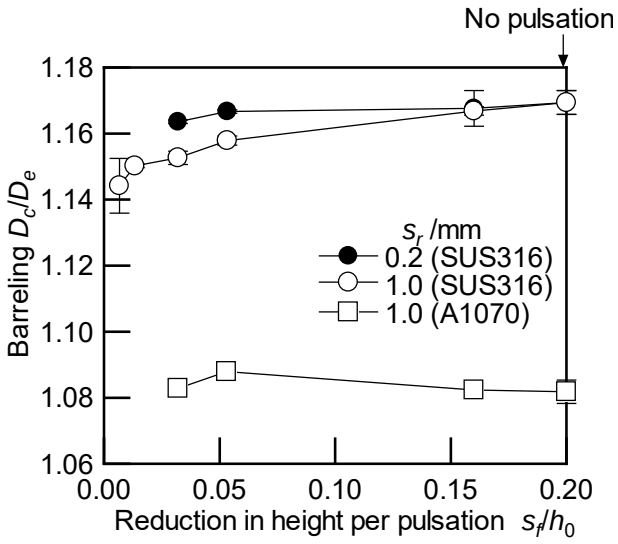

Fig. 7 Relationship between barreling and forming stroke per pulsation after upsetting with $s_{total}/h_0 = 0.20$.

3.2 Load–stroke relationship

Figure 8 shows the load–reduction in height relationship in upsetting of the stainless steel workpiece. Although upsetting was proceeded with repeating loading and unloading in pulsation ram motion, the load during deformation of the workpiece was almost the same with/without ram pulsation. From the load–reduction in height relationship in **Figure 8**, the load fraction at the re-start of forming and the start of ram retreat in upsetting with ram pulsation is shown in **Figure 9**. The load fraction was lower than 1.0 in upsetting with reduction in barreling (stainless steel workpiece with s_r = 1.0 mm), while the load fraction was higher than 1.0 in no reduction in barreling (stainless steel workpiece with s_r = 0.2 mm and aluminum workpiece). Thus, the load reduction at re-start of forming (reloading) may influence on the reduction in barreling.

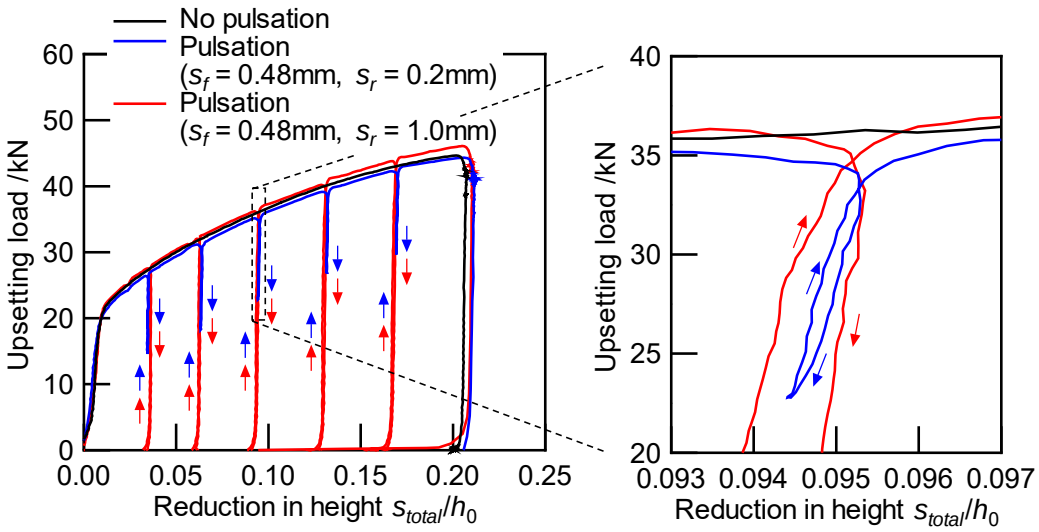

Fig. 8 Load–reduction in height relationship in upsetting of stainless steel workpiece.

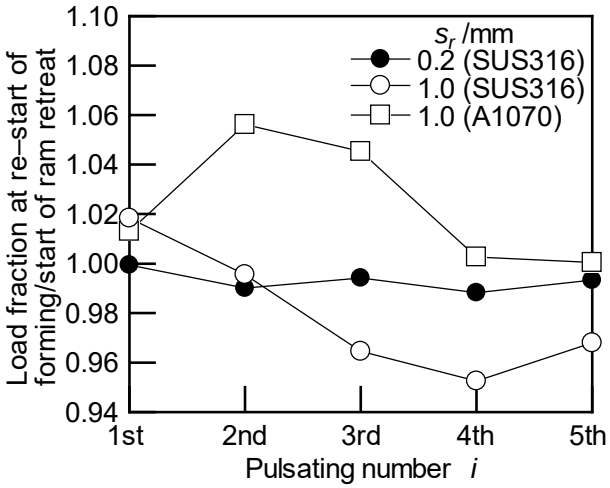

Fig. 9 Load fraction at start of reloading/unloading in upsetting with ram pulsation (s_f = 0.48 mm).

4. Discussions on reduction in barreling

4.1. Friction and temperature rise

Barreling is strongly affected by friction at the die–workpiece contact interface and temperature change of the workpiece during deformation. **Figure 10** shows the photographs of the die surface after upsetting. Seizure and adhesion of the workpiece were not observed on

the die surface in upsetting with/without ram pulsation. The difference in friction at the die–workpiece contact interface was small in upsetting with/without ram pulsation.

The temperature rise of the stainless steel workpiece by plastic deformation in upsetting was estimated by the finite element analysis. The maximum temperature rise was approximately 25 K without ram pulsation and 20 K with ram pulsation at $s_{total}/h_0 = 0.20$. The influence of the temperature difference of 5 K on the deformation behavior could be generally disregarded, especially around room temperature.

From above discussions, reduction in barreling of the stainless steel workpiece in upsetting with complete unload pulsation is concluded not to be due to differences of friction and temperature rise with/without ram pulsation.

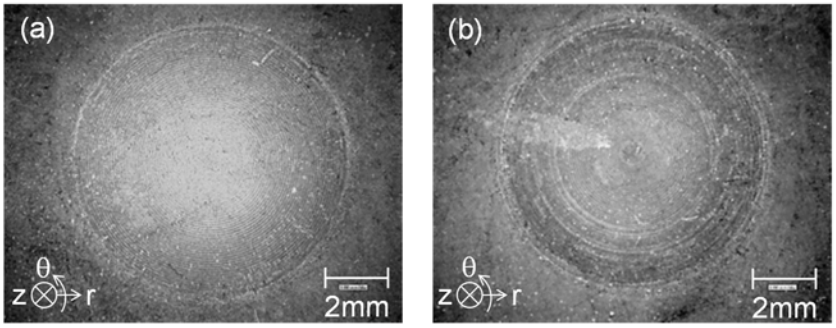

Fig. 10 Photographs of die surface after upsetting of stainless steel workpiece with $s_{total}/h_0 = 0.20$: (a) no ram pulsation, (b) ram pulsation with $s_f = 0.48$ mm, $s_r = 1.0$ mm.

4.2. Elastic-plastic deformation

4.2.1. Finite element analysis conditions

The elastic-plastic deformation of the workpiece in upsetting with/without ram pulsation was numerically calculated by a commercial elastic-plastic finite element code, Simufact Forming ver. 16.0 (MSC Software Company). The analysis model is shown in **Figure 11**. Two-dimensional axisymmetric deformation was assumed from the consideration

of shape symmetry. The workpiece was treated as elastic-plastic body with isothermal, while the dies were treated as elastic bodies with isothermal. The element type of the workpiece and the dies was a quadrilateral 4-node element with sides of 0.20 mm. The elements were not remeshed. The material properties of the stainless steel and the pure aluminum at room temperature were used. The flow stress–strain relationship was assumed to be isotropic hardening, and the strain rate sensitivity on the flow stress was not taken into account. According to the Swift law, the following flow stress–strain relationships measured by the upsettability test [31,32] of cylindrical workpiece were used.

(stainless steel) $\sigma = 994(\varepsilon + 0.005)^{0.336}$ (MPa) (2)

(pure aluminum) $\sigma = 148(\varepsilon + 0.005)^{0.195}$ (MPa) (3)

On the assumption of Coulomb's friction law, the friction coefficient was set to 0.1 on the die–workpiece contact interface.

Figure 12 shows the analysis and experimental results of the load–stroke curve and barreling in upsetting without ram pulsation. Good agreements between the analysis and experimental results were obtained in the load–stroke curve and barreling. Thus, the material properties used in the analysis were confirmed to be suitable.

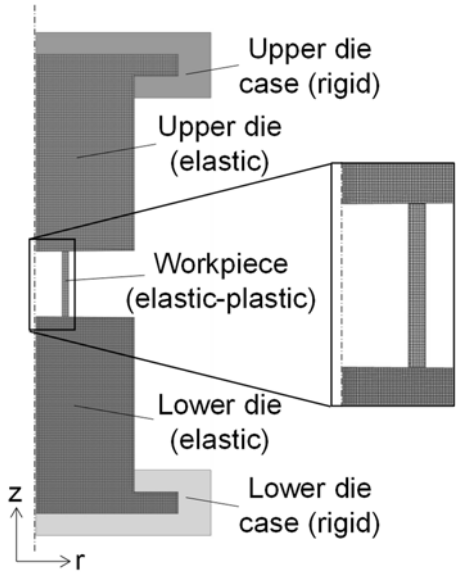

Fig. 11 Finite element analysis model for elastic-plastic deformation of hollow cylindrical workpiece in upsetting with/without ram pulsation.

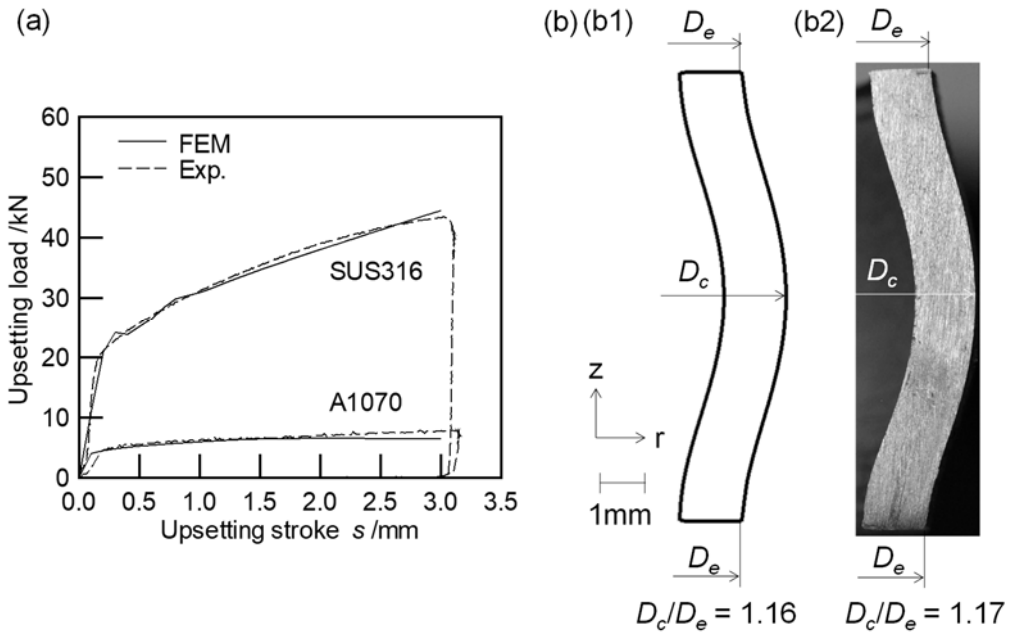

Fig. 12 Comparison of analysis and experimental results of (a) load–stroke curve and (b) barreling in upsetting of stainless steel workpiece without ram pulsation (s_{total} = 3.0 mm): (b1) FEM, (b2) experiment.

4.2.2. Finite element analysis results

Figure 13 shows the shape of the stainless steel workpiece at the finish of 1st ram retreat in upsetting. The height of the workpiece increased with increasing retreat stroke, while the radius of the workpiece at the height center decreased. The deformations were due to elastic recovery by the ram retreat. The z-normal stress distribution of the stainless steel workpiece during the 1st ram retreat in upsetting is shown in **Figure 14**. Here, the stress/proof stress ($\sigma/\sigma_{0.2}$) during the ram retreat was -1.48–0.47 in z direction, while $\sigma/\sigma_{0.2}$ in r and θ directions were -0.19–0.45 and -0.74–0.89, respectively. The r- and θ-normal stresses were absolutely lower than the proof stress ($\sigma_{0.2}$ = 371 MPa). The z-normal stress was compressive in all area of the section in s_r = 0–0.2 mm (partial unloading), while it was reversed from compressive to tensile in almost half area of the section at s_r = 1.0 mm (complete unloading). The area faction of the tensile z-normal stress in the section (α) was 0 in s_r = 0–0.2 mm and 0.53 at s_r = 1.0 mm. After then the z-normal stress was reversed again from tensile to compressive at the re-start of forming. On the other hand, the $\sigma_z/\sigma_{0.2}$ distribution of the pure aluminum workpiece during the ram retreat was almost the same with that of the stainless steel, α = 0 in s_r = 0–0.2 mm and α = 0.48 at s_r = 1.0 mm.

From the consideration of the above stress change, the stress distributions at the re-start of forming and the start of the ram retreat were different in complete unload ram retreat. Since it is known that stainless steel exhibits Bauschinger effect [33], the flow stress after stress reversal nominally decreases at re-start of forming. As the results, the deformation behavior of the stainless steel workpiece after the re-start of forming in complete unload ram retreat was different with that in incomplete unload ram retreat. Therefore, barreling of the stainless steel workpiece was reduced by compete unload pulsation. The decrease of the flow stress at re-start of forming was experimentally confirmed that the load fraction was lower than 1.0 in upsetting of SUS316 workpiece with complete unload pulsation as shown in

Figure 9. On the other hand, although the stress distribution of the pure aluminum workpiece was almost the same with that of the stainless steel workpiece, barreling of the pure aluminum workpiece was not reduced in complete unload pulsation. This is because pure aluminum does not clearly exhibit Bauschinger effect [33].

Figure 15 shows the analysis and experimental results of the load–stroke curve in upsetting with complete unload pulsation. Since the flow stress of the workpiece was employed to isotropic hardening law in the analysis, the flow stress did not decrease after the re-start of forming. Good agreement in the load–stroke curves between the analysis and experimental results was obtained in the pure aluminum workpiece, while the load–stroke curve of the analysis was slightly higher than of the experiment in the stainless steel workpiece.

From the above discussions, reduction in barreling in upsetting with ram pulsation is concluded to be due to combination of stress reversal under complete unload ram retreat and Bauschinger effect.

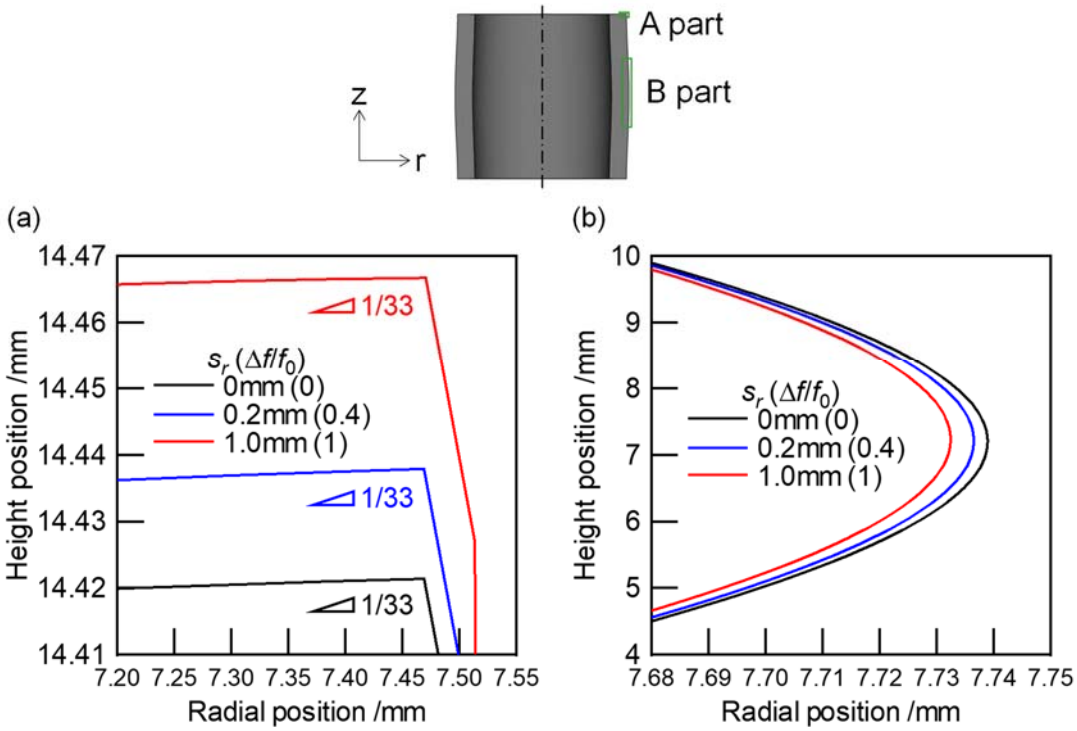

Fig. 13 Shape of stainless steel workpiece at finish of 1st ram retreat in upsetting with s_{total} = 0.6 mm (FEM): (a) outer edge at top end (A part), (b) outer shape (B part).

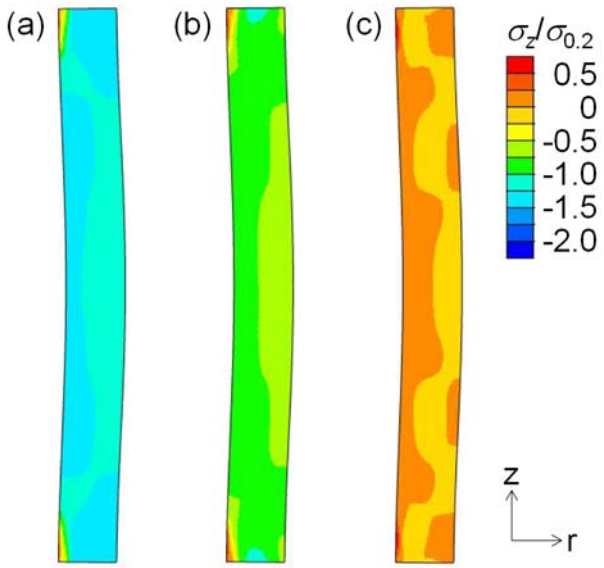

Fig. 14 z-normal stress distribution of stainless steel workpiece in rz longitudinal section during 1st ram retreat in upsetting with s_{total} = 0.6 mm (proof stress: $\sigma_{0.2}$ = 371 MPa, FEM): (a) s_r = 0 mm ($\Delta f/f_0$ = 0), (b) s_r = 0.2 mm ($\Delta f/f_0$ = 0.4), (c) s_r = 1.0 mm ($\Delta f/f_0$ = 1).

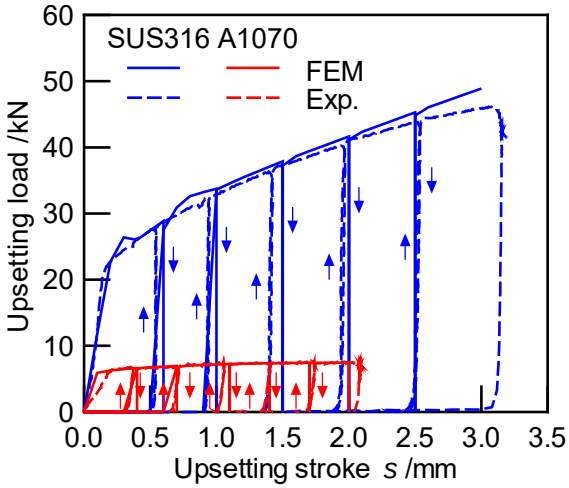

Fig. 15 Comparison of analysis and experimental results of load–stroke curve in upsetting with complete unload pulsation.

5. Conclusions

In this study, barreling of hollow cylinder in cold upsetting with ram pulsation was investigated with experiment and finite element analysis. The ram pulsation has a potential of new forming technique for reducing barreling in forming of hollow cylinder. The following remarks were obtained.

(1) In upsetting of stainless steel workpiece, barreling was reduced by approximately 2.5% in maximum under complete unload ram pulsation, especially under multiple pulsations with short stroke. On the other hand, barreling was reduced under ram pulsation in upsetting of pure aluminum workpiece.

(2) In complete unload ram pulsation, z-normal stress was reversed from compression to tension during ram retreat. The stress state at re-start of forming after unloading was different with that of no ram pulsation. Due to the Bauschinger effect after stress reversal, the deformation behaviors of the stainless steel workpiece were different with/without complete unload ram pulsation. Therefore, the reduction in barreling in upsetting with

complete unload ram pulsation was concluded to be mainly due to the elastic-plastic characteristic of the stainless steel workpiece.

Acknowledgement

This work was financially supported in part by the Amada Foundation (AF-2022006-B2).

Declaration of conflicts of interest

The authors declare no competing interests.

Authors' contributions

Ryo Matsumoto: Conceptualization, Methodology, Formal analysis, Investigation, Data Curation, Visualization, Writing - Original Draft, Supervision

Yuya Monda: Investigation, Data Curation

Hiroshi Utsunomiya: Validation, Writing - Review & Editing

References

[1] Kleiner M, Geiger M, Klaus A (2003) Manufacturing of lightweight components by metal forming. CIRP Annals – Manufacturing Technology 52(2): 521–542. https://doi.org/10.1016/S0007-8506(07)60202-9

[2] Zhao X, Wu H, Zhang Z (2016) A new rolling-extrusion technology for the forming of the hollow cylindrical component. International Journal of Advanced Manufacturing Technology 86(1-4): 1127–1136. https://doi.org/10.1007/s00170-016-8573-9

[3] Guo X, Wang C, Xu Y, El-Aty A (2019) Incremental forming characteristics of hollow parts with grooves. International Journal of Advanced Manufacturing Technology

102(1-4): 829–837. https://doi.org/10.1007/s00170-018-3201-5

[4] Neugebauer R, Glaß R, Hoffmann M, Putz M (2005) Incremental forming of hollow shapes. Steel Research International 76(2): 171–176. https://doi.org/10.1002/srin.200505991

[5] Winiarski G, Gontarz A, Samołyk G (2020) Theoretical and experimental analysis of a new process for forming flanges on hollow parts. Materials 13(18): 4088. https://doi.org/10.3390/ma13184088

[6] Osakada K, Mori K (1986) A study of buckling in upsetting by use of finite element method. CIRP Annals – Manufacturing Technology 35(1): 161–164. https://doi.org/10.1016/S0007-8506(07)61861-7

[7] Gariety M, Ngaile G (2005) Friction and lubrication. Cold and Hot Forging: Fundamentals and Applications (Altan T, Ngaile G, Shen G eds.). ASM International: 67–81. ISBN: 978-0-87170-805-2

[8] Mori K, Maeno T, Maki S (2007) Mechanism of improvement of formability in pulsating hydroforming of tubes. International Journal of Machine Tools and Manufacture 47(6): 978–984. https://doi.org/10.1016/j.ijmachtools.2006.07.006

[9] Tatematsu Y, Morimoto M, Kitamura K (2018) Experiment and FE analysis of compression of thick ring filled with oil. Key Engineering Materials 767: 141–148. https://doi.org/10.4028/www.scientific.net/KEM.767.141

[10] Matsumoto R, Tanaka S, Utsunomiya H (2022) Enhancement of plastic flow in lateral direction by torsional oscillation in upsetting and lateral extrusion. Journal of Materials Processing Technology 299: 117369. https://doi.org/10.1016/j.jmatprotec.2021.117369

[11] Matsumoto R, Tanaka S, Utsunomiya H (2024) Reduction in barreling of hollow cylinder by combination of axial compression and circumferential torsion in upsetting

with conical dies. Proceedings of the 14th International Conference on the Technology of Plasticity - Current Trends in the Technology of Plasticity. Lecture Notes in Mechanical Engineering 1: 27–35. https://doi.org/10.1007/978-3-031-41023-9_3

[12] Khoddam S, Fardi M, Solhjoo S (2021) A verified solution of friction factor in compression test based on its sample's shape changes. International Journal of Mechanical Sciences 193: 106175. https://doi.org/10.1016/j.ijmecsci.2020.106175

[13] Ebrahimi R, Najafizadeh A (2004) A new method for evaluation of friction in bulk metal forming. Journal of Materials Processing Technology 152(2): 136–143. https://doi.org/10.1016/j.jmatprotec.2004.03.029

[14] Solhjoo S, Khoddam S (2019) Evaluation of barreling and friction in uniaxial compression test: A kinematic analysis. International Journal of Mechanical Sciences 156: 486–493. https://doi.org/10.1016/j.ijmecsci.2019.04.007

[15] Yao Z, Mei D, Shen H, Chen Z (2013) A friction evaluation method based on barrel compression test. Tribology Letters 51: 525–535. https://doi.org/10.1007/s11249-013-0164-4

[16] Wang X, Li H, Chandrashekhara K, Rummel SA, Lekakh S, Van Aken DC, O'Malley RJ (2017) Inverse finite element modeling of the barreling effect on experimental stress-strain curve for high temperature steel compression test. Journal of Materials Processing Technology 243: 465–473. http://dx.doi.org/10.1016/j.jmatprotec.2017.01.012

[17] Li YP, Onodera E, Matsumoto H, Chiba A (2009) Correcting the stress-strain curve in hot compression process to high strain level. Metallurgical and Materials Transactions A 40(4): 982–990. https://doi.org/10.1007/s11661-009-9783-7

[18] Villié L, Cabrol E, Hof L, Feulvarch E, Bocher P (2023) Heterogeneities induced by uniaxial compression and resulting errors in material behavior assessment. International Journal of Material Forming 16(5): 58. https://doi.org/10.1007/s12289-023-01782-z

[19] Khoddam S, Mansourinejad M, Mirzakhani B, Hodgson PD, Taylor AS (2022) A comprehensive experimental and numerical study of foldover onset and growth during the barrelling compression test. Advances in Mechanical Engineering 14(12): 1–16. https://doi.org/10.1177/16878132221143873

[20] Osakada K, Mori K, Altan T, Groche P (2011) Mechanical servo press technology for metal forming. CIRP Annals – Manufacturing Technology 60(2): 651–672. https://doi.org/10.1016/j.cirp.2011.05.007

[21] Halicioglu R, Dulger LC, Bozdana AT (2017) Modeling, design, and implementation of a servo press for metal-forming application. The International Journal of Advanced Manufacturing Technology 91(5-8): 2689–2700. https://doi.org/10.1007/s00170-016-9947-8

[22] Yamamoto H, Wadabayashi R (1970) Forward extrusion with oscillation. Proceedings of the 21st Japanese Joint Conference for the Technology of Plasticity: 439–442. (in Japanese)

[23] Matsumoto R (2024) A review of oscillation forging. Proceedings of the 9th JSTP International Seminar on Precision Forging (ISPF 2024): 83–90.

[24] Maeno T, Osakada K, Mori K (2011) Reduction of friction in compression of plates by load pulsation. International Journal of Machine Tools and Manufacture 51(7-8): 612–617. https://doi.org/doi: 10.1016/j.ijmachtools.2011.03.007

[25] Matsumoto R, Sawa S, Utsunomiya H, Osakada K (2011) Prevention of galling in forming of deep hole with retreat and advance pulse ram motion on servo press. CIRP Annals – Manufacturing Technology 60(1): 315–318. https://doi.org/10.1016/j.cirp.2011.03.147

[26] Matsumoto R, Nakamura Y, Utsunomiya H (2023) *In situ* observation of re-lubrication of die–workpiece interface during forging with ram pulsation. Journal of

Manufacturing Processes 101: 675–686. https://doi.org/10.1016/j.jmapro.2023.06.017

[27] Matsumoto R, Jeon JY, Utsunomiya H. (2013) Shape accuracy in the forming of deep holes with retreat and advance pulse ram motion on a servo press. Journal of Materials Processing Technology 213(5): 770–778. https://doi.org/10.1016/j.jmatprotec.2012.11.023

[28] Ishikawa T, Ishiguro T, Yukawa N, Goto T (2014) Control of thermal contraction of aluminum alloy for precision cold forging. CIRP Annals – Manufacturing Technology 63(1): 289–292. https://doi.org/10.1016/j.cirp.2014.03.008

[29] Hariharan K, Majidi O, Kim C, Lee MG, Barlat F (2013) Stress relaxation and its effect on tensile deformation of steels. Materials and Design: 52, 284–288. https://doi.org/10.1016/j.matdes.2013.05.088

[30] Majidi O, Barlat F, Lee, MG (2016) Effect of slide motion on springback in 2-D draw bending for AHSS. International Journal of Material Forming: 9(3), 313–326. https://doi.org/10.1007/s12289-014-1214-7

[31] Osakada K, Kawasaki T, Mori K (1981) A method of determining flow stress under forming conditions. CIRP Annals – Manufacturing Technology: 30(1), 135–138. https://doi.org/10.1016/S0007-8506(07)60910-X

[32] Kudo H, Sato K, Aoi K (1968) A cold upsettability test. CIRP Annals – Manufacturing Technology: 16(4), 309–318.

[33] Yilamu K, Hino R, Hamasaki H, Yoshida F (2010) Air bending and springback of stainless steel clad aluminum sheet. Journal of Materials Processing Technology: 210(2), 272–278. https://doi.org/10.1016/j.jmatprotec.2009.09.010